Jokiniemi, Kimi; Ryynänen, Kaisa; Vähä, Joni; Stadius, Kari; Ryynänen, Jussi

Analysis of Current-Commutating Passive and Active Mixers for mmWave Applications

Published in:
ISCAS 2024 - IEEE International Symposium on Circuits and Systems

DOI:
10.1109/ISCAS58744.2024.10558149

Published: 01/01/2024

Document Version
Peer-reviewed accepted author manuscript, also known as Final accepted manuscript or Post-print

Analysis of Current-Commutating Passive and Active Mixers for mmWave Applications

Kimi Jokiniemi, Kaisa Ryynänen, Joni Vähä, Kari Stadius, Jussi Ryynänen
Department of Electronics and Nanoengineering, Aalto University, Finland
Email: kimi.jokiniemi@aalto.fi

***Abstract*—This paper analyses and compares key differences between active and passive mixer structures in the context of mmWave applications. Firstly, the paper analyses mixer switching stage input impedance and its implications on frequency response. Active mixers provide isolation, whereas passive switching entails impedance transparency beneficial for filtering. Secondly, the paper analyses mixer performance with a low-amplitude sinusoidal LO signal typical for mmWave frequencies. Such an LO signal entails partly overlapping, unideal switching. However, active switching transistors commutate current more ideally during the overlap stage, demonstrating superior sinusoidal LO signal tolerance. Importantly, this work demonstrates that despite multiple passive mixer benefits, their performance is highly dependent on the LO signal. Finally, based on the analysis, the paper introduces a wideband active mmWave downconversion mixer design in 22-nm FDSOI CMOS. Measured characteristics demonstrate a particularly wide bandwidth of 55 to 100 GHz.**

***Index Terms*—microwave integrated circuits, CMOS, active mixer, passive mixer, sinusoidal LO signal**

I. Introduction

The growth of wireless communication systems and sensing applications have increased the demand for wireless millimeter wave (mmWave) radio systems. The mmWave frequency band between 30 GHz and 300 GHz has become increasingly prospective due to its availability of wide, continuous communication bands and still relatively small usage enabling high data rate communications and increased concurrent user capabilities [1]. The maturing of CMOS technologies have further rendered mmWave integrated systems compelling as the well-established technology can offer better availability, lower manufacturing costs, higher level of integration, and now increasingly competitive performance with more conventional high-frequency compound semiconductor technologies [2].

Mixers perform frequency conversion and are a key component in radio transceiver systems. However, a key challenge at mmWave frequencies is the inability to generate an ideal square wave local oscillator (LO) signal to drive the mixer, due to their requirement for multiple strong harmonic frequencies. These frequencies are heavily attenuated in mmWave circuits typically aiming to operate near the frequency limits of semiconductor devices, and thus LO signals are often limited to a sinusoidal waveform. Hence, especially N-path mixer designs with below 50% LO duty cycles, which are favored at sub-6-GHz bands [3], [4], become unfeasible. High-frequency nanometer processes also generally provide low intrinsic gain [5] and use low supply voltages, posing limitations for linearity. These mmWave design challenges entail issues of varying significance for passive and active mixers.

The remainder of this article is organized as follows. Firstly, Section II elaborates on the classification of mixers and analyses passive and active mixer switching stage input impedance and its implications on mixer performance. The section continues with the analysis of passive and active mixer performance when driven by a sinusoidal LO signal. Then, Section III introduces an active CMOS mixer implementation for 55-100 GHz [6] based on the analysis. Lastly, Section IV concludes the paper by summarizing the essential achievements.

II. Analysis

A. Mixer Classification

Mixers typically consist of a transconductance stage performing V-I conversion, a current switching stage performing frequency conversion, and a load performing I-V conversion. A crucial distinction between active and passive mixers is the operation of the switching stage transistors. Passive switching transistors alternate operating region between cutoff region and linear region, operating as voltage-controlled switches. Contrarily, active switching transistors switch operating region between cutoff and saturation, drawing DC current and functioning as common-gate amplifiers when conducting [7]. Passive switching stages are often combined with active, amplifying V-I and I-V stages, which are often not considered part of the passive mixer [3], [8]. However, reported active mixer designs typically comprise all three stages [9], [10], possibly leading to unfair comparison. Thus, mixer classification and analysis in this paper focuses on the switching transistors.

B. Input Impedance

The input impedance of the switching stage is critical for mixer frequency response as it forms the input pole, dictating the radio frequency (RF) band. Low switching stage input impedance is desired to maximize downconversion mixer RF input bandwidth and minimize voltage swings. Fig. 1 illustrates double-balanced mixer switches, which depending on the biasing, can be either active or passive. Switching stage input impedance is denoted as Z_{IN} and lumped parasitic capacitance as C_P. The following input impedance analysis is performed in the context of downconversion mixers.

In an active mixer, the resistive input impedance is simply equal to the inverse of switching transistor transconductance,

$$Z_{IN,Active} = 1/g_{m,sw}, \tag{1}$$

disregarding channel length modulation and parasitic coupling. This is because each input node is ideally connected to the source node of exactly one switching transistor operating in saturation at all times [11]. Therefore, the input pole is formed at a frequency $\omega = g_{m,sw}/C_P$. The active mixer intermediate frequency (IF) output bandwidth is dictated by Z_L, and the input impedance and thus the RF band is ideally independent of the load impedance. The reverse isolation provided by an active switching stage reduces port-to-port signal leakage and enables independent RF domain and IF domain stage design.

In a passive mixer, load impedance Z_L is visible at the switching stage input with frequency translation and scaling because switching stage input voltage forms as follows. First, the RF current signal passes through the switching stage and is frequency-translated. The output current then forms a voltage over the load impedance in the IF domain. The passive mixer functions reciprocally, so the IF output voltage signal is converted back to the RF domain propagating in the reverse direction and forming the switching stage input voltage. Thus, as derived in [12] and [13], the single-ended input impedance is given by the equation

$$Z_{IN,Passive}(\omega_{RF}) = R_{sw} + \frac{4}{\pi^2} \cdot \sum_{n=1,3,5...}^{\infty} \left(\frac{1}{n^2} \cdot \Big(Z_L(\omega_{RF} - n\omega_{LO}) + Z_L(\omega_{RF} + n\omega_{LO}) \Big) \right). \quad (2)$$

The switch resistance term R_{sw} is present because each input ideally sees exactly one switching transistor drain to source resistance at all times. The factor $4/\pi^2$ is the double-balanced switching stage current conversion gain (CG) squared, resulting from the signal passing through the switching stage twice [13]. The downconversion mixer load impedance typically has a low-pass characteristic to attenuate frequencies outside the desired IF signal band. In this case, spurious frequency terms with $n > 1$ and also the upconverted term at $\omega_{RF} + \omega_{LO}$ can be discarded as they are typically well outside of the IF band in mmWave systems. Hence, a low-pass impedance at the passive mixer output is translated to a band-pass impedance centered around f_{LO} at the switching stage input, resulting in

$$Z_{IN,Passive}(\omega_{RF}) \approx R_{sw} + \frac{4}{\pi^2} Z_L(\omega_{RF} - \omega_{LO}). \quad (3)$$

Neglecting R_{sw} and assuming a low IF frequency further simplifies the equation to

$$Z_{IN,Passive}(\omega_{RF}) \approx \frac{4}{\pi^2} R_L. \quad (4)$$

In this case, the input pole is formed at a frequency $\omega = \pi^2/(4C_P R_L)$. This RF and IF stage mutual dependence reduces some design freedom, however, the impedance frequency translation can be leveraged to implement tunable high-Q RF filters challenging to implement otherwise [14].

C. Sinusoidal LO Signal Performance

The LO signal drives the switching transistors and commutates input current through alternating branches to perform

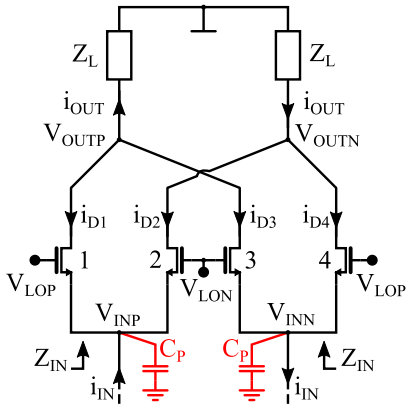

Fig. 1: Double-balanced mixer switching transistors.

frequency conversion. Ideally, current commutation happens abruptly between branches but a sinusoidal LO signal typical for mmWave frequencies entails an overlap time around the LO signal zero-crossings. During this overlap time, the switching transistors of both branches, i.e. both transistors in pairs 1 and 2 as well as 3 and 4 in Fig. 1, conduct simultaneously. Overlap time decreases conversion gain and increases output noise. Fig. 2 illustrates the overlap periods in active and passive mixers with a sinusoidal LO signal.

Active mixer switching transistors are simultaneously in saturation region and operate as a differential pair during the overlap time. The switching transistor pair commutates most of the tail current through one branch even before one of the transistors switches off fully, reducing the effective overlap time. It can be approximated that the currents flowing through the branches of a differential pair are equal and no differential output current is created when $|V_{LO}| < (V_{GS} - V_{tn})_{eq}/5$, and that outside of this differential pair input voltage range, the pair commutates the tail current solely through one branch as is ideal [11]. Hence, mixer output current is the product of input current i_{IN} and effective LO signal $x(t)$ varying between values 1,0, and -1.

With a sinusoidal LO signal, the ratio of total effective active mixer overlap time and LO signal period is derived as

$$2V_{p,LO} \cdot \sin\left(\omega_{LO} \frac{T_{Overlap,Active}}{4}\right) = \frac{(V_{GS} - V_{tn})_{eq}}{5} \quad (5)$$

$$\frac{T_{Overlap,Active}}{T_{LO}} = \frac{2}{\pi} \cdot \sin^{-1}\left(\frac{(V_{GS} - V_{tn})_{eq}}{10V_{p,LO}}\right). \quad (6)$$

In the equations, $(V_{GS} - V_{tn})_{eq}$ is the switching transistor overdrive voltage at equilibrium, and $V_{p,LO}$ is the single-ended LO signal peak value. Active mixer conversion gain accounting for the overlap time caused by a sinusoidal LO signal is achieved by multiplying the abrupt switching conversion gain $\frac{2}{\pi}$ by a factor of $\cos\left(\frac{\pi}{2}\frac{T_{Overlap}}{T_{LO}}\right)$ derived from the Fourier analysis of $x(t)$ [12]. With trigonometry, this factor can be transformed into the final active mixer conversion gain equation

$$CG_{Active} = \frac{2}{\pi}\sqrt{1 - \left(\frac{(V_{GS} - V_{tn})_{eq}}{10V_{p,LO}}\right)^2}. \quad (7)$$

The equation solely expresses the current conversion gain in the switching transistors without the contribution of additional mixer stages. The equation also disregards parasitic circuit elements for simplicity. The equation is valid for $V_{p,LO}/(V_{GS}-V_{tn})_{eq} \geq 0.1$ and $CG_{Active} = 0$ otherwise.

Gradual switching due to a sinusoidal LO signal has an even more harmful effect on passive mixer performance. In passive current-mode mixers, the switching transistors are typically biased so that $V_{GS,eq} > V_{tn}$ to avoid presenting an open circuit for the current-mode input at any stage [15]. Nevertheless, equal overlap time is formed when $V_{GS,eq} < V_{tn}$. As illustrated in Fig. 2, the tail current commutation is minimal when all passive mixer transistors are simultaneously in linear region. Thus, unlike in active mixers, the passive mixer effective overlap stage lasts for the entire period when all transistors are conducting, i.e., when $|V_{LO}| < 2(V_{GS}-V_{tn})_{eq}$. Performing the same analysis as in the active mixer case, the ratio of total passive mixer overlap time and the LO signal period can be derived as

$$2V_{p,LO} \cdot \sin\left(\omega_{LO}\frac{T_{Overlap,Passive}}{4}\right) = 2(V_{GS}-V_{tn})_{eq} \quad (8)$$

$$\frac{T_{Overlap,Passive}}{T_{LO}} = \frac{2}{\pi} \cdot \sin^{-1}\left(\frac{(V_{GS}-V_{tn})_{eq}}{V_{p,LO}}\right). \quad (9)$$

Thus, passive mixer switching stage current conversion gain with a sinusoidal LO signal can be expressed as

$$CG_{Passive} = \frac{2}{\pi}\sqrt{1-\left(\frac{(V_{GS}-V_{tn})_{eq}}{V_{p,LO}}\right)^2}, \quad (10)$$

which is valid for $V_{p,LO}/(V_{GS}-V_{tn})_{eq} \geq 1$ and $CG_{Passive} = 0$ otherwise.

D. Discussion

A commonly used approximation in the CG calculation is $\sin(\omega_{LO}T_{overlap}/4) \approx \omega_{LO}T_{overlap}/4$ [11]. This approximation is only accurate when $T_{overlap}$ is small compared to T_{LO}. Additionally, as a linear approximation to achieve gradual switching conversion gain, abrupt switching conversion gain can be multiplied by a factor of $1 - T_{overlap}/T_{LO}$, which yields a simple formula but sacrifices accuracy. Therefore, the presented equations (5)–(10) avoid these approximations.

Fig. 3 presents an analytical comparison of passive and active mixer current conversion gains with a sinusoidal LO signal. The x axis is the ratio of single-ended LO signal amplitude and switching transistor equilibrium overdrive voltage. Active mixer demonstrates superior gain performance with a low-amplitude LO signal and the analytical effective overlap time period is up to 15.7 times larger in a passive mixer than in an active mixer with identical LO signal characteristics. However, equilibrium overdrive voltage can be reduced in passive mixers to reduce the LO level demand [16]. Active mixers, on the contrary, inherently require overdrive voltage to bias the switches in saturation. Both switching stage classes provide equal abrupt switching conversion loss and thus, gain

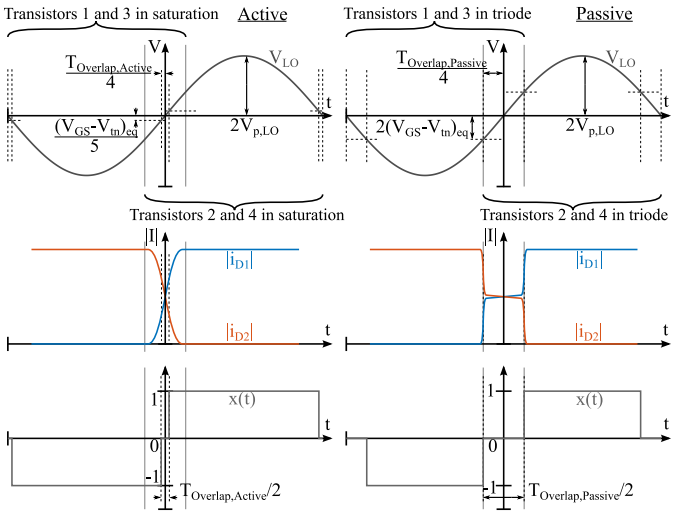

Fig. 2: Illustration of active and passive mixer overlap time periods, drain current commutation, and effective LO signals.

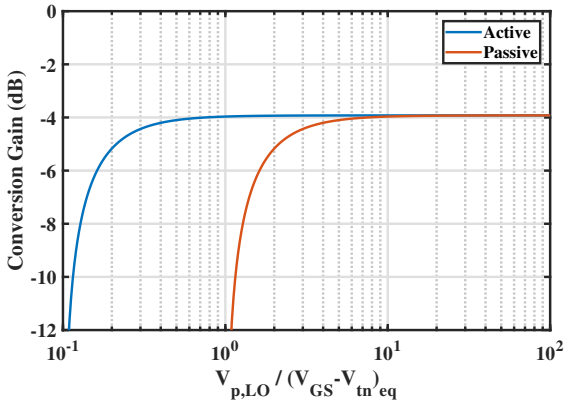

Fig. 3: Analytical values for active and passive switching conversion gain with identical LO signal characteristics.

comparison is irrelevant when focusing solely on the actual mixing stage [15].

Overlap time also degrades noise performance in both mixer classes. Qualitatively analysed, passive switch white noise is proportional to R_{sw}, which is inversely proportional to switch $V_{gs}-V_{tn}$. Notably, during overlap, $V_{gs}-V_{tn}$ is low and both passive switches simultaneously contribute to output noise. Active switches can contribute white noise to the output only during the overlap period [17]. Passive switches lack flicker noise [9], whereas the output flicker noise contribution of active switching transistors is caused by the switch flicker noise modulating the switching instant, and so is inversely proportional to sinusoidal LO signal slope and thus, LO signal amplitude at a constant f_{LO} [17].

As for linearity, the voltage swings at the passive mixer input may alter the switching instant nonlinearly especially with a weak LO signal, while the switching instant in active mixers always happens at the LO zero-crossing due to the differential pair operation [15]. Active mixer switching stage

input voltage swings should not exceed voltage headroom limits to avoid compression yet nevertheless, active mixer linearity qualitatively displays lower dependence on LO signal.

III. Active mmWave Mixer Implementation

The presented analysis on the lower LO signal demand in active mixers has motivated the design of an active mmWave downconversion mixer [6]. The proposed modified Gilbert cell mixer structure combined with a common-source LO buffer and a two-stage IF amplifier has been fabricated in 22-nm FDSOI CMOS. The mixer schematic is presented in Fig. 4 and the fabricated chip is presented in Fig. 5. The designed mixer has interstage transformer coupling between the switching and transconductance stages of the mixer. Transformer coupling introduces peaking inductance and decouples the mixer stages at DC improving voltage headroom and allowing individual stage biasing. A lower bias current is used in the switching stage to lower the overdrive voltage of the switching transistors enabling more abrupt switching and lowering flicker noise [11], [18]. As analyzed, this also increases switching stage input impedance, posing a tradeoff for RF bandwidth. This effect is countered by the peaking inductance, which resonates out parasitic capacitance at the switching stage input nodes within the RF band [10].

The mixer demonstrates a particularly wide measured RF frequency band of 55–100 GHz (58% fractional bandwidth) covering a range of mmWave bands with a single device. The peak voltage conversion gain is 3.5 dB as presented in Fig. 6. The IF output band extends from 100 MHz up to 10 GHz supporting large, multi-GHz channel bandwidths. The entire mixer consumes 33 mW of power from a particularly low 0.8 V supply voltage. The mixer core area is 0.13 mm^2 disregarding input baluns and contact pads used for measuring.

IV. Conclusion

This paper has compared passive and active mixers in the context of mmWave systems focusing on two key distinctions. Firstly, active switching transistors provide isolation whereas passive transistors entail impedance transparency and frequency translation. Thus, the RF and IF stages are independent of each other only in an active mixer, restricting passive mixer design freedom, yet the impedance frequency translation in passive mixers may be leveraged for RF filtering. Secondly, a low-amplitude sinusoidal LO signal typical for mmWave frequencies causes overlapping switching decreasing multiple mixer performance aspects. Active mixers minimize the effective overlap time, leading to superior tolerance for a low-amplitude sinusoidal LO signal. This work demonstrates that whereas passive mixers consume no DC power, have high linearity, and lack flicker noise, their performance is highly dependent on the LO signal level. Lastly, the paper has briefly proposed an active mmWave downconversion mixer with interstage transformer coupling implemented in 22-nm FDSOI CMOS. The mixer structure achieves a measured peak conversion gain of 3.5 dB, a wide RF frequency band of 55-100 GHz and a wide IF bandwidth of 10 GHz.

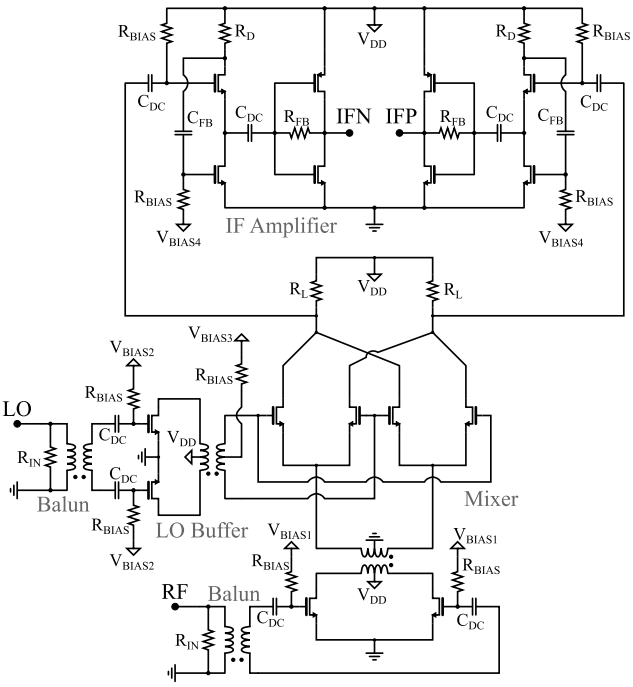

Fig. 4: Proposed active mixer schematic.

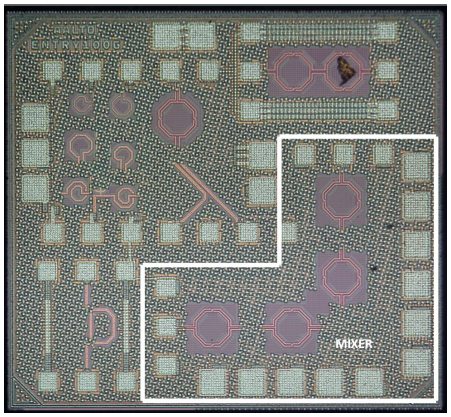

Fig. 5: Microphotograph of an IC die with mmWave circuits. The outlined mixer occupies an active area of 0.13 mm^2.

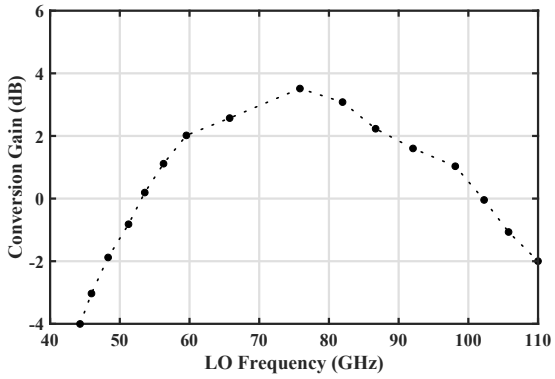

Fig. 6: Measured mixer conversion gain with f_{IF}=1 GHz.

REFERENCES

[1] A. M. Niknejad and H. Hashemi, *mm-Wave Silicon Technology: 60 GHz and Beyond*, 1st ed. New York, NY: Springer, 2008.

[2] P. Testa, V. Rieß, C. Carta, and F. Ellinger, "An Inductorless 60GHz Down-Conversion Mixer in 22nm FD-SOI CMOS Technology," in *2019 14th European Microwave Integrated Circuits Conference (EuMIC)*, 2019, pp. 152–155.

[3] Z. G. Boynton and A. Molnar, "A 9-31GHz 65nm CMOS Down-Converter with ¿4dBm OOB B1dB," in *2020 IEEE Radio Frequency Integrated Circuits Symposium (RFIC)*, 2020, pp. 279–282.

[4] C. Andrews and A. C. Molnar, "Implications of Passive Mixer Transparency for Impedance Matching and Noise Figure in Passive Mixer-First Receivers," *IEEE Transactions on Circuits and Systems I: Regular Papers*, vol. 57, no. 12, pp. 3092–3103, 2010.

[5] S. Juneja, R. Pratap, and R. Sharma, "Semiconductor technologies for 5G implementation at millimeter wave frequencies – Design challenges and current state of work," *Engineering Science and Technology, an International Journal*, vol. 24, no. 1, pp. 205–217, 2021.

[6] K. Jokiniemi, K. Ryynänen, J. Vähä, E. Kankkunen, K. Stadius, and J. Ryynänen, "Active wideband 55-100-ghz downconversion mixer in 22-nm fdsoi cmos," in *2023 IEEE Nordic Circuits and Systems Conference (NorCAS)*, 2023, pp. 1–7.

[7] A. Molnar and C. Andrews, "Impedance, filtering and noise in n-phase passive CMOS mixers," in *Proceedings of the IEEE 2012 Custom Integrated Circuits Conference*, 2012, pp. 1–8.

[8] R. van de Beek, J. Bergervoet, H. Kundur, D. Leenaerts, and G. van der Weide, "A 0.6-to-10GHz Receiver Front-End in 45nm CMOS," in *2008 IEEE International Solid-State Circuits Conference - Digest of Technical Papers*, 2008, pp. 128–601.

[9] M. Voltti, T. Koivisto, and E. Tiiliharju, "Comparison of active and passive mixers," in *2007 18th European Conference on Circuit Theory and Design*, 2007, pp. 890–893.

[10] Y.-S. Lin and Y. E. Wang, "Design and Analysis of a 94-GHz CMOS Down-Conversion Mixer With CCPT-RL-Based IF Load," *IEEE Transactions on Circuits and Systems I: Regular Papers*, vol. 66, no. 8, pp. 3148–3161, 2019.

[11] B. Razavi, *RF Microelectronics*, 2nd ed. Upper Saddle River, NJ: Pearson, 2011.

[12] H. Darabi, *Radio Frequency Integrated Circuits and Systems*, 1st ed. Cambridge, United Kingdom: Cambridge University Press, 2015.

[13] H. Khatri, P. S. Gudem, and L. E. Larson, "Distortion in Current Commutating Passive CMOS Downconversion Mixers," *IEEE Transactions on Microwave Theory and Techniques*, vol. 57, no. 11, pp. 2671–2681, 2009.

[14] P. K. Sharma and N. Nallam, "Linearity and NF Tradeoff in Input-Matched N-Path Mixer-First Receivers with Shunt-Feedback TIAs," in *2019 IEEE International Symposium on Circuits and Systems (ISCAS)*, 2019, pp. 1–4.

[15] S. Chehrazi, A. Mirzaei, and A. A. Abidi, "Noise in Current-Commutating Passive FET Mixers," *IEEE Transactions on Circuits and Systems I: Regular Papers*, vol. 57, no. 2, pp. 332–344, 2010.

[16] V. Issakov, D. Siprak, M. Tiebout, A. Thiede, W. Simburger, and L. Maurer, "Comparison of 24 GHz receiver front-ends using active and passive mixers in CMOS," *Circuits, Devices & Systems, IET*, vol. 3, pp. 340 – 349, 01 2010.

[17] H. Darabi and A. Abidi, "Noise in RF-CMOS mixers: a simple physical model," *IEEE Journal of Solid-State Circuits*, vol. 35, no. 1, pp. 15–25, 2000.

[18] D.-H. Seo, J.-Y. Lee, and T.-Y. Yun, "Active and Passive Combined Mixer for Low Flicker Noise and Low dc Offset," *IEEE Microwave and Wireless Components Letters*, vol. 25, no. 7, pp. 463–465, 2015.